DESY 16-101

Exploring the nearly degenerate stop region with sbottom decays

Haipeng An,[a,1] **Jiayin Gu,**[b,c,2] **Lian-Tao Wang** [d,e,3]

[a] *Walter Burke Institute for Theoretical Physics, California Institute of Technology, Pasadena, CA 91125.*

[b] *Center for Future High Energy Physics, Institute of High Energy Physics, Chinese Academy of Sciences, Beijing 100049, China.*

[c] *DESY, Notkestraße 85, D-22607 Hamburg, Germany.*

[d] *Enrico Fermi Institute, University of Chicago, Chicago, IL 60637.*

[e] *Kavli Institute for Cosmological Physics, University of Chicago, Chicago, IL 60637.*

Abstract

A light stop with mass almost degenerate with the lightest neutralino has important connections with both naturalness and dark matter relic abundance. This region is also very hard to probe at colliders. In this paper, we demonstrate the potential of searching for such stop particles at the LHC from sbottom decays, focusing on two channels with final states $\boldsymbol{2\ell + E_T^{miss}}$ and $\boldsymbol{1b1\ell + E_T^{miss}}$. We found that, if the lightest sbottom has mass around or below 1 TeV and has a significant branching ratio to decay to stop and W ($\tilde{b} \to \tilde{t}\, W$), a stop almost degenerate with neutralino can be excluded up to about 500–600 GeV at the 13 TeV LHC with 300 fb^{-1} data. The searches we propose are complementary to other SUSY searches at the LHC and could have the best sensitivity to the stop-bino coannihilation region. Since they involve final states which have already been used in LHC searches, a reinterpretation of the search results already has sensitivity. Further optimization could deliver the full potential of these channels.

[1] anhp@caltech.edu

[2] jiayin.gu@desy.de

[3] liantaow@uchicago.edu

Contents

1 Introduction

A light stop is essential for the naturalness of supersymmetry (SUSY). The stops have been extensively searched at the LHC. Traditional searches focus on the direct production of a stop pair followed by each stop decaying to the top quark and the lightest neutralino, $\tilde{t} \to t\,\chi$, while the lightest neutralino χ is the lightest superpartner (LSP). The signal of these searches often includes large missing transverse momentum ($E_{\mathrm{T}}^{\mathrm{miss}}$) from the LSP. The current LHC bound for R-parity conserving SUSY models on stop mass is around $m_{\tilde{t}} \gtrsim 900\,\mathrm{GeV}$, assuming $\tilde{t} \to t\,\chi$ and a sufficiently large mass gap between $m_{\tilde{t}}$ and m_χ [1–11].[1]

The stops can still be significantly lighter than this bound if they are hiding in compressed regions $m_{\tilde{t}} \approx m_t + m_\chi$, $m_{\tilde{t}} \approx m_W + m_b + m_\chi$ and $m_{\tilde{t}} \approx m_\chi$, in which cases it is hard to discriminate the stop signal from standard model (SM) backgrounds or the products of the stop decay is too soft to be identified. Based on the stop-neutralino simplified model, searching strategies have been proposed to search for stops in these regions [12–59]. In R-parity conserving SUSY, the $m_{\tilde{t}} \approx m_\chi$ region is of special interests if the neutralino χ is mainly composed by the bino $\tilde{B}$. The reason is that the annihilation cross section of a pair of $\tilde{B}$ is small due to the lack of gauge interaction. Therefore, for $\tilde{B}$ to be a thermal dark matter candidate, a charged particle must be nearby to assist the annihilation. This region is thus called stop-bino coannihilation region [60]. This region is also not very well

[1] Stop may also decay to the lightest neutralino via an intermediate chargino or heavier neutralino, in which case the bounds on the stop mass is slightly weaker.

constrained by dark matter direct detection experiments [61]. According to the numerical simulation with micrOmegas4.2 [62], for sub-TeV bino-like dark matter, a mass difference $m_{\tilde{t}_1} - m_\chi \approx 30\,\text{GeV}$ is required to obtain the measured relic abundance. In the simulations of this work, we fix this mass gap to be 30 GeV. The sensitivities of collider search discussed in this paper are slightly better if the mass gap is smaller. In this compressed region, the stop has two main decay channels, one is the flavor-conserving four-body decay through off-shell top quark and W boson ($\tilde{t} \to bW^*\chi \to bl\nu\chi/bjj\chi$) and the other is the flavor-changing two-body decay to a charm quark ($\tilde{t} \to c\,\chi$). The decay rate of the flavor-changing channel depends strongly on the flavor structure of the squark sector, whereas the rate of the four-body channel depends only on the mixing angle between the left and right handed stop. It turns out that with $m_{\tilde{t}_1} - m_\chi = 30\,\text{GeV}$, the four-body channel alone makes the stop decay promptly [47].

In this paper, we draw attention to a couple of additional useful search channels using sbottom decays, to further probe this nearly degenerate region. Naturalness prefers the second stop not to be too heavy. Due to the doublet nature of the left handed quarks, the masses of the left handed sbottom is connected to the mass of the left handed stop. The mixing between the left and right handed stops usually makes the mass of the second stop heavier than the left handed sbottom. To minimize the flavor violation induced by the squark sector, the mixing between the left and right handed sbottoms is usually assumed to be suppressed by the mass of the bottom quark. Therefore, we can decouple the right handed sbottom in this work. Our search strategy relies on a significant mass gap between the lightest stop and sbottom, which we obtain by assuming $m_{\tilde{t}_R}$ is sufficiently smaller than $m_{\tilde{t}_L} (= m_{\tilde{b}_L})$, and the lightest stop is mostly right-handed. [2] To simplify the study we also assume the winos and the Higgsinos are decoupled and the lightest neutralino is pure bino. The spectrum of the SUSY particles is shown in Fig. 1. In this simplified scenario, the lighter sbottom $\tilde{b}_1$ has two decay channels

$$\begin{aligned} \tilde{b}_1 &\to W + \tilde{t}_1 \,, \\ \tilde{b}_1 &\to b + \chi \,, \end{aligned} \tag{1.1}$$

[2] A large mass gap could also be generated by a very large stop A term even if $m_{\tilde{t}_R} \approx m_{\tilde{t}_L}$, but with such a large A term also comes the risk of spontaneously breaking $SU(3)_c$. In this scenario, the decay $\tilde{b} \to \tilde{t}\,W$ would dominate which makes our case even stronger.

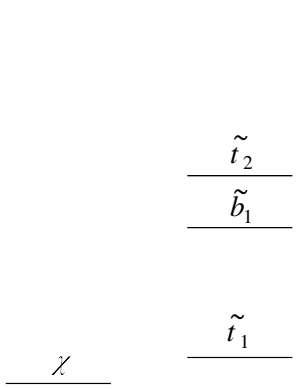

Figure 1: Spectrum of SUSY partners of the stop-bino coannihilation region.

with decay rates

$$\begin{aligned}
\Gamma_1 &\equiv \Gamma_{\tilde{b}_1 \to W \tilde{t}_1} = \frac{g_2^2 \sin^2\theta_t \cos^2\theta_b}{32\pi} \frac{[(m_{\tilde{b}}^2 - (m_{\tilde{t}} + m_W)^2)(m_{\tilde{b}}^2 - (m_{\tilde{t}} - m_W)^2)]^{3/2}}{m_W^2 m_{\tilde{b}}^3} \ , \\
\Gamma_2 &\equiv \Gamma_{\tilde{b}_1 \to b \chi} = \frac{g_1^2}{32\pi} \frac{(m_{\tilde{b}}^2 - m_\chi^2)^2}{m_{\tilde{b}}^3} 4 \left[\left(-\frac{1}{3}\right)^2 \sin^2\theta_b + \left(\frac{1}{6}\right)^2 \cos^2\theta_b \right] \ ,
\end{aligned} \tag{1.2}$$

where in calculating Γ_2 we neglect the mass of the bottom quark. The stop and sbottom mixing angles are defined as

$$\begin{pmatrix} \tilde{t}_1 \\ \tilde{t}_2 \end{pmatrix} = \begin{pmatrix} \cos\theta_t & \sin\theta_t \\ -\sin\theta_t & \cos\theta_t \end{pmatrix} \begin{pmatrix} \tilde{t}_R \\ \tilde{t}_L \end{pmatrix} \ , \qquad \begin{pmatrix} \tilde{b}_1 \\ \tilde{b}_2 \end{pmatrix} = \begin{pmatrix} \cos\theta_b & \sin\theta_b \\ -\sin\theta_b & \cos\theta_b \end{pmatrix} \begin{pmatrix} \tilde{b}_L \\ \tilde{b}_R \end{pmatrix} \ . \tag{1.3}$$

In the limit $m_{\tilde{b}}^2 - m_{\tilde{t}}^2 \gg m_W^2$, Γ_1 is seemingly enhanced by the factor $m_{\tilde{b}}^2/m_W^2$ due to the longitudinal contribution. However, the stop mixing angle vanishes if the electroweak symmetry is unbroken. Therefore, the stop mixing angle θ_t is secretly proportional to m_W. In the limit $A_t v \ll m_{\tilde{t}_2}^2 \approx m_{\tilde{b}}^2$, we have

$$\sin\theta_t \approx \frac{\sqrt{2} A_t m_W}{g_2 m_{\tilde{b}}^2} \ , \tag{1.4}$$

where A_t is the A term for the stops. Assuming A_b is suppressed by m_b for the sake of flavor physics constraints, we have $\cos\theta_b \approx 1$. Therefore, Γ_1 and Γ_2 in Eq. (1.2) can be simplified as

$$\Gamma_1 \approx \frac{A_t^2}{16\pi m_{\tilde{b}}} \ , \quad \Gamma_2 \approx \frac{\alpha_{\rm em} m_{\tilde{b}}}{72 \cos^2\theta_W} \ . \tag{1.5}$$

The proportionality of Γ_1 to A_t^2 can also be inferred from the goldstone equivalence theorem. The traditional sbottom search based on the sbottom-neutralino simplified model

assumes the sbottom decays 100% to b and the neutralino. However, as from Eq. (1.5) if A_t is comparable to $m_{\tilde{b}}$, Γ_1/Γ_2 can be as large as $\mathcal{O}(100)$. This region is also favored by the Higgs mass. On the other hand, in some specific SUSY breaking models (e.g. gauge mediation models) A_t is one-loop order suppressed compared to other soft SUSY breaking parameters. In this case, $\Gamma_1 \ll \Gamma_2$. Therefore, when searching for the signal from sbottoms, it is important to consider both of the two decay channels.

We will focus on studying the potential of the sbottom decay channels shown in **(a)** and **(b)** of Fig. 2. We apply relatively straightforward cuts to demonstrate that these channels can lead to interesting reach with an integrated luminosity of 300 fb^{-1} at the 13 TeV LHC. A more careful optimization of the kinematical selection and more realistic simulation are needed to determine the ultimate reach. This is beyond the scope of this paper. We also present the reach in the more "conventional" sbottom search channel in shown in **(c)** of Fig. 2 to illustrate the complementarity between these channels. We would like to emphasize that even in the parameter region in which **(c)** has a better reach, the new channels **(a)** and **(b)** studied in this paper is still useful in the case of a discovery since they directly probe the presence of the stop.

The rest of this paper is organized as follows: In Section 2, we discuss the main search channels and the corresponding backgrounds. In Section 3, we state the selection cuts for each channel and show the results of a few case studies. In Section 4, we show the exclusion regions in the parameter space of the 13 TeV LHC with 300 fb^{-1} data and compare the reaches of different channels. The conclusion is drawn in Section 5.

2 Search channels and backgrounds

With two decay channels $\tilde{b} \to \tilde{t}\,W$ and $\tilde{b} \to b\,\chi$,[3] a pair of sbottoms produced at the LHC has three ways to decay, as shown in Fig. 2. The symmetric decay chain of $\tilde{b} \to b\,\chi$ in Fig. 2c has already been searched at the LHC in the channel with final states $\boldsymbol{2b + E_T^{miss}}$ under the assumption of 100% branching ratio (BR), and sbottom with mass up to 800 GeV are excluded for $m_\chi \lesssim 360$ GeV [63]. With a smaller branching ratio, the reach of this channel is significantly weaker. Here our main interest is in the decay chains that involves the stop, namely, the symmetric decay chain in Fig. 2a and the asymmetric decay chain in Fig. 2b. As such, we will focus on two channels, one with final states of two opposite sign leptons and $E_{\rm T}^{\rm miss}$ ($\boldsymbol{2\ell + E_T^{miss}}$), and the other with one hard b-jet, one lepton

[3] In this paper $\tilde{t}$ and $\tilde{b}$ always denote the lighter mass eigenstates, $\tilde{t}_1$ and $\tilde{b}_1$, unless specified otherwise.

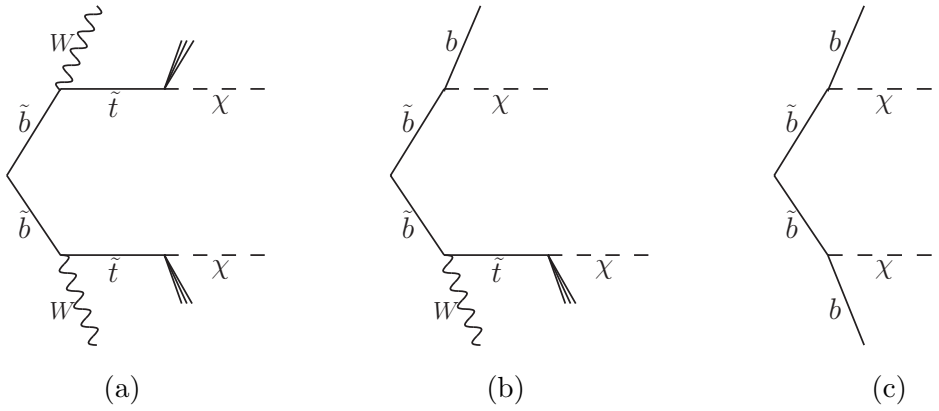

Figure 2: Three ways for a sbottom pair to decay for the scenario studied in this paper: **(a)** symmetric decay of $\tilde{b} \to \tilde{t}\,W$, **(b)** asymmetric decay, and **(c)** symmetric decay of $\tilde{b} \to b\,\chi$.

and $E_{\rm T}^{\rm miss}$ ($\boldsymbol{1b1\ell + E_{\rm T}^{\rm miss}}$). These two channels are studied in details in Section 3, while in Section 4 we compare their reaches together with the one of the $\boldsymbol{2b + E_{\rm T}^{\rm miss}}$ channel for different sbottom branching ratios.

The $\boldsymbol{2\ell + E_{\rm T}^{\rm miss}}$ channel is designed to pick up the the symmetric decay chain in Fig. 2a with both Ws decaying leptonically, and should be the optimal search channel if the decay $\tilde{b} \to \tilde{t}\,W$ dominates. This channel has been searched at the LHC for the searches of sleptons and electroweakinos [64, 65], for which the main background is top quark pair production ($t\bar{t}$) and diboson ($WW/WZ/ZZ$). We also found the $t\bar{t}Z$ events to have a significant contribution to the SM backgrounds after imposing our selection cuts.

The $\boldsymbol{1b1\ell + E_{\rm T}^{\rm miss}}$ channel is designed for the asymmetric decay chain in Fig. 2b, but could also pick up some events from the symmetric decay chain in Fig. 2a with one W decaying hadronically, if the event happens to have a hard b-jet. This channel is similar to the direct search of stop pair in the semileptonic channel [6, 7, 11], where the main backgrounds include $t\bar{t}$, tW, $W+$jets, diboson and ttZ. We expect this channel to be useful if the branching ratios of $\tilde{b} \to \tilde{t}\,W$ and $\tilde{b} \to b\,\chi$ are comparable.

In principle, one could also search in the channel with final states of one lepton, $E_{\rm T}^{\rm miss}$ and one or two hard jets with no b-jets ($\boldsymbol{1\ell + \text{jets} + E_{\rm T}^{\rm miss}}$), which could come from either Fig. 2a with one W decaying hadronically or Fig. 2b if the b-jet is not tagged. While this channel could contain significant amount of signal events, the backgrounds are also large and more complicated. In this paper, we focus on the simpler leptonic channels as an initial assessment of the potential of these new decay channels.

signal	σ[pb]	$m_{\tilde{b}}$[GeV]	$m_{\tilde{t}}$[GeV]	m_{χ}[GeV]	BR($\tilde{b} \to \tilde{t}\,W$)	$\tilde{t}$ decay
S1	0.00615	1000	600	570	0.9	$c\,\chi$
S2	0.00615	1000	600	570	0.9	$bl\nu\chi/bjj\chi$
S3	0.0129	900	500	470	0.5	$c\,\chi$
S4	0.0129	900	500	470	0.5	$bl\nu\chi/bjj\chi$

Table 1: Signal samples used for the case studies in the $\boldsymbol{2\ell + E_{\mathrm{T}}^{\mathrm{miss}}}$ channel (S1 & S2) and the $\boldsymbol{1b1\ell + E_{\mathrm{T}}^{\mathrm{miss}}}$ channel (S3 & S4).

3 Simulation procedure and event selection

For both signal and backgrounds, the events are generated at parton level using Madgraph5 [66], followed by parton showering with PYTHIA6.4 [67]. The detector simulation is performed with Delphes [68] in which the b-tagging efficiency is from [69]. We use the above procedure to generate the events of sbottom pair production and then rescale the cross section to the values from the NLO+NLL calculation in Ref. [70, 71]. For $t\bar{t}$, single top and W, Z+jets events the MLM matching procedure is also employed, and for the $t\bar{t}$ events the total cross section is scaled to the NNLO+NNLL result given in Ref. [72, 73]. For diboson events, the total cross section is scaled to the NLO result in Ref. [74]. For $t\bar{t}Z$ events, we scale the cross section to the central value of the recent measurement in Ref. [75].

We present the details of our collider study in this section, including the selection cuts for each channel and the results of a few case studies. The signal samples listed Table 1 are used for the case studies. Signal S1 & S2 has BR($\tilde{b} \to \tilde{t}\,W$) = 0.9 and are ideal for the $\boldsymbol{2\ell + E_{\mathrm{T}}^{\mathrm{miss}}}$ channel, while S3 & S4 has BR($\tilde{b} \to \tilde{t}\,W$) = 0.5 which is better covered by the $\boldsymbol{1b1\ell + E_{\mathrm{T}}^{\mathrm{miss}}}$ channel. For S1 & S3, we assume the stop only decays to charm and neutralino, $\tilde{t} \to c\,\chi$; for S2 & S4, we assume that the stop only goes through the 4-body decay, $\tilde{t} \to bW^*\chi \to bl\nu\chi/bjj\chi$. The mass spectra in Table 1 are chosen to roughly correspond to the "best reach" of the two channels, which are shown later in Section 4.

3.1 $\boldsymbol{2\ell + E_{\mathrm{T}}^{\mathrm{miss}}}$ channel

Selection cuts: For an event to pass the cut, we require it to have $E_{\mathrm{T}}^{\mathrm{miss}} > 150\,\mathrm{GeV}$ and contain exactly 2 leptons with opposite charge. We require the scalar sum of the p_T of the two leptons to be larger than 200 GeV. We also apply a b-veto by requiring the event to have no b-jet with $p_T > 50\,\mathrm{GeV}$. The requirement on p_T of b-jets could prevent one

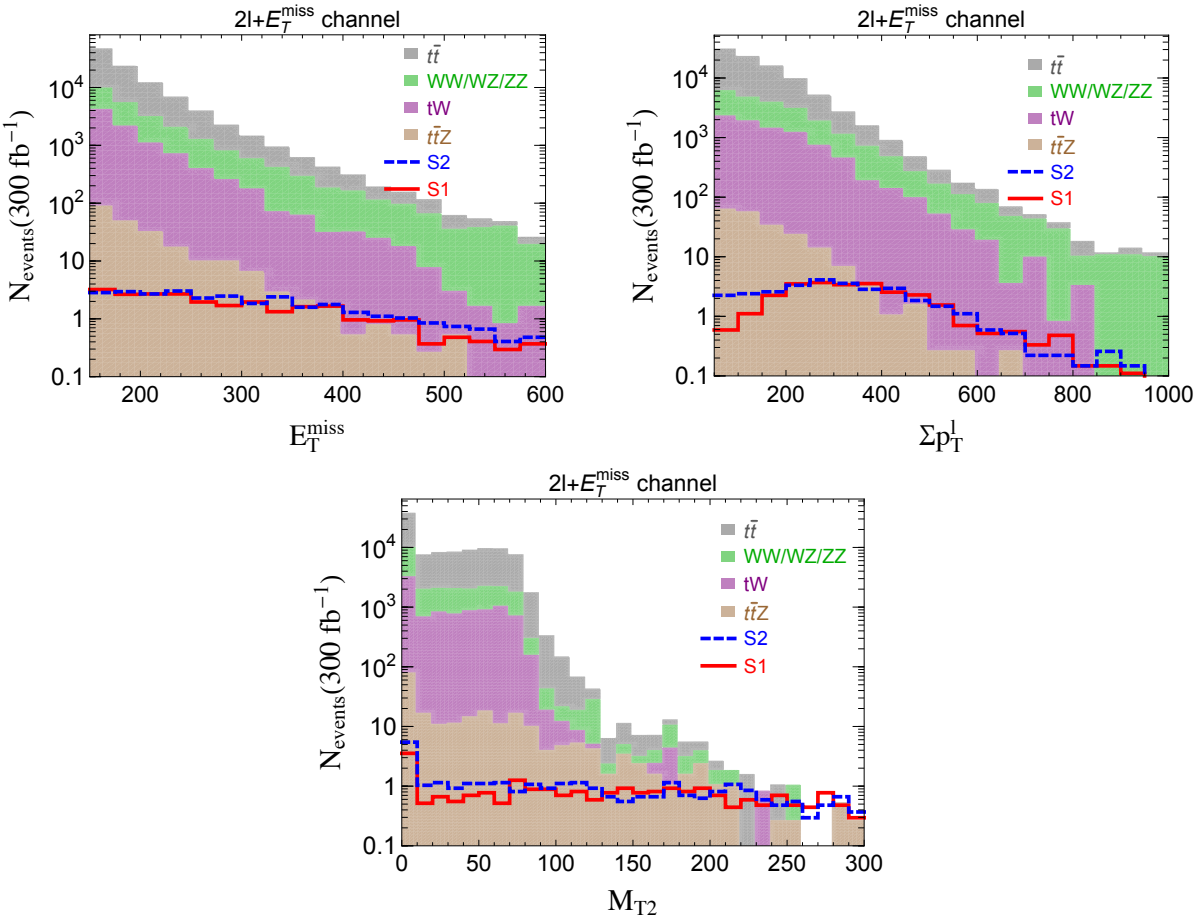

Figure 3: Distributions of $E_{\mathrm{T}}^{\mathrm{miss}}$ (**top left**), $\sum p_T^l$ (**top right**) and M_{T2} (**bottom**) of the $\boldsymbol{2\ell + E_{\mathrm{T}}^{\mathrm{miss}}}$ channel for signal sample S1 and the major backgrounds. $\sum p_T^l$ is the scalar sum of the p_T of the two leptons. To illustrate the usefulness of the variables, the cuts $\{\sum p_T^l > 200\,\mathrm{GeV}\ ,\ M_{\mathrm{T2}} > 150\,\mathrm{GeV}\}$ are removed. The number of events correspond to $300\,\mathrm{fb}^{-1}$ at the 13 TeV LHC.

from removing signal events with soft b-jets from stop decays. We require the invariant mass of the lepton pair (m_{ll}) to be larger than 20 GeV to remove potential backgrounds from low mass resonances. If the two leptons have the same flavor, we further require their invariant mass to be at least 20 GeV away from the Z boson mass. A stringent cut around the Z resonance helps remove the ZZ background with $ZZ \to \ell^+\ell^-\nu\bar{\nu}$, which cannot be efficiently removed by the M_{T2} variable due to the different event topology. In order to remove events with a large $E_{\mathrm{T}}^{\mathrm{miss}}$ coming from mis-measurements of jet energy, we require that the azumithal angle between the missing transverse momentum and any jet with $p_T > 50\,\mathrm{GeV}$ to satisfy $|\phi_{\mathrm{MET}} - \phi_j| > 0.2$. Finally, we require the M_{T2} of the lepton pair to be larger than 150 GeV.

	# of events ($300\,\mathrm{fb}^{-1}$)	$s/\sqrt{b}$
S1	13	2.0
S2	12	2.0
$t\bar{t}$	11	
$WW/WZ/ZZ$	15	
$t\bar{t}Z$	8.4	
tW	5.1	
total SM	40	

Table 2: Number of events of signal and backgrounds and the corresponding $s/\sqrt{b}$ after all of the selection cuts for the $\boldsymbol{2\ell + E_{\mathrm{T}}^{\mathrm{miss}}}$ channel with $300\,\mathrm{fb}^{-1}$ data. The details of signal samples S1 & S2 are listed in Table 1. All the generated backgrounds are included in the row "total SM."

The distributions of $E_{\mathrm{T}}^{\mathrm{miss}}$, $\sum p_T^l$ (scalar sum of the p_T of the two leptons) and M_{T2} are shown in Fig. 3 for signal S1, S2 and the major backgrounds. In Fig. 3 one could clearly see the endpoint feature of the M_{T2} distribution of the $t\bar{t}$, $WW/WZ/ZZ$ and tW backgrounds. [4] A cut on M_{T2} with a value much larger than the W mass is very efficient at removing these backgrounds. On the other hand, the $t\bar{t}Z$ background has additional neutrinos and does not have the endpoint feature. While it has a much smaller cross section, after the M_{T2} cut we found it to be comparable with other major backgrounds. The numbers of signals and backgrounds after the selection cuts and the corresponding $s/\sqrt{b}$ for $300\,\mathrm{fb}^{-1}$ data are shown in Table 2. Comparing the results of S1 and S2, one could see that the decay channel of the light stop has a rather small impact on the reach, due to the high jet and lepton threshold we choose to use.

3.2 $\boldsymbol{1b1\ell + E_{\mathrm{T}}^{\mathrm{miss}}}$ channel

Selection cuts: We require the event to have $E_{\mathrm{T}}^{\mathrm{miss}} > 350\,\mathrm{GeV}$ and contain exactly one lepton, one b-jet with $p_T > 150\,\mathrm{GeV}$ and no additional b-jet with $p_T > 50\,\mathrm{GeV}$. To remove events with large $E_{\mathrm{T}}^{\mathrm{miss}}$ due to mis-measurements of jet energy, we require $|\phi_{\mathrm{MET}} - \phi_j| > 0.3$ for any jet with $p_T > 100\,\mathrm{GeV}$. We require the transverse mass of the lepton $M_T > 200\,\mathrm{GeV}$ in order to remove backgrounds of which the dominate source of missing energy is from the leptonically decaying W (*e.g.* semileptonic $t\bar{t}$). Finally, we require the variable M_{T2}^W reconstructed from the event to be at least $200\,\mathrm{GeV}$. An event

[4] Note that most ZZ background are removed by the lepton invariant mass cut. If this cut is not imposed, a significant amount of ZZ background will have $M_{\mathrm{T2}} \gtrsim m_W$.

	# of events ($300\,\text{fb}^{-1}$)	$s/\sqrt{b}$
S3	35	1.8
S4	43	2.2
$t\bar{t}$	207	
$W+$jets	84	
tW	43	
$WW/WZ/ZZ$	28	
$t\bar{t}Z$	26	
total SM	389	

Table 3: Number of events of signal and backgrounds and the corresponding $s/\sqrt{b}$ after all of the selection cuts for the $\boldsymbol{1b1\ell + \not{E}_{\mathrm{T}}^{\mathrm{miss}}}$ channel with $300\,\text{fb}^{-1}$ data. The details of signal samples S3 & S4 are listed in Table 1. All the generated backgrounds are included in the row "total SM."

is also kept if it does not contain any additional jet for M_{T2}^W to be constructed.

The variable M_{T2}^W, proposed in Ref [76], is constructed for dileptonic $t\bar{t}$ background with one lepton not reconstructed, and has been shown to be useful in suppressing this type of background [7, 9].[5] The calculation of M_{T2}^W requires one to identify the two b-jets and to know which one is on the same side as the visible lepton. In practice, one does not have this knowledge and would usually calculate the M_{T2}^W for different possible combinations and output the minimum value from these combinations. Here we assume the other b-jet is among the three leading non-b-tagged jets. We then choose the combination which minimizes M_{T2}^W.

The distributions of $E_{\mathrm{T}}^{\mathrm{miss}}$, p_T^b, M_{T} and M_{T2}^W are shown in Fig. 4 for signal S1 and the major backgrounds. For the M_{T2}^W distribution, events for which $M_{\mathrm{T2}}^W > 1\,\text{TeV}$ are stacked on the last bin. The usefulness of M_{T2}^W can be seen in Fig. 4, as the number of background events, in particular for $t\bar{t}$, falls sharply with M_{T2}^W above the top mass. The numbers of signals and backgrounds after the selection cuts and the corresponding $s/\sqrt{b}$ for $300\,\text{fb}^{-1}$ data are shown in Table 3. For the $\boldsymbol{1b1\ell + \not{E}_{\mathrm{T}}^{\mathrm{miss}}}$ channel, the reach is also not very sensitive to the decay channel of stop.

[5] Other variables have also been proposed for suppressing this background, such as am_{T2} [77] and *topness* [78]. As their performances are somewhat similar, for simplicity we only use M_{T2}^W in this paper.

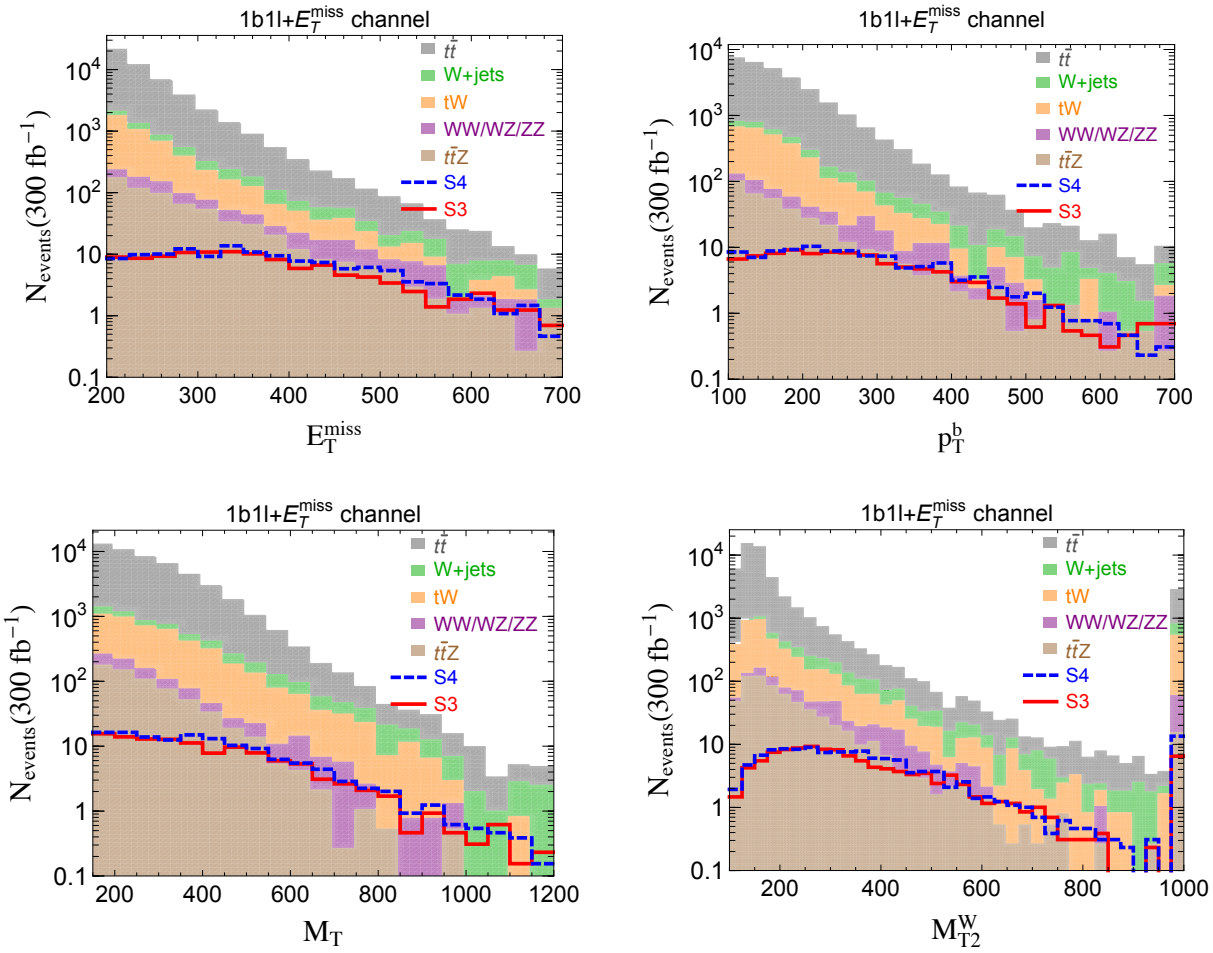

Figure 4: Distributions of $E_{\mathrm{T}}^{\mathrm{miss}}$ (**top left**), p_T^b (**top right**), M_{T} (**bottom left**) and M_{T2} (**bottom right**) of the $\boldsymbol{1b1\ell + E_{\mathrm{T}}^{\mathrm{miss}}}$ channel for signal sample S3 and the major backgrounds. To illustrate the usefulness of the variables, the cuts $\{E_{\mathrm{T}}^{\mathrm{miss}} > 350\,\mathrm{GeV}$, $p_T^b > 150\,\mathrm{GeV}$, $M_{\mathrm{T}} > 200\,\mathrm{GeV}$, $M_{\mathrm{T2}}^W > 200\,\mathrm{GeV}\}$ are replaced by looser cuts $\{E_{\mathrm{T}}^{\mathrm{miss}} > 200\,\mathrm{GeV}$, $p_T^b > 50\,\mathrm{GeV}$, $M_{\mathrm{T}} > 150\,\mathrm{GeV}$, $M_{\mathrm{T2}}^W > 0\,\mathrm{GeV}\}$. For the M_{T2}^W distribution, events for which M_{T2}^W cannot be constructed below 1 TeV are stacked on the last bin. The number of events correspond to $300\,\mathrm{fb}^{-1}$ at the 13 TeV LHC.

4 Reach at the 13 TeV LHC

We scan over the signal parameter space to determine the reach of the $\boldsymbol{2\ell + E_T^{miss}}$ and $\boldsymbol{1b1\ell + E_T^{miss}}$ channels at the 13 TeV LHC, assuming an integrated luminosity of $300\,\text{fb}^{-1}$. For comparison, we also include the results of the conventional search channel of the sbottom, $\boldsymbol{2b + E_T^{miss}}$, which has the best reach if the dominant decay of sbottom is $\tilde{b} \to b\,\chi$. To estimate the reach of the $\boldsymbol{2b + E_T^{miss}}$ channel, we adopt the cuts in Ref. [63] for signal region **SRA450**, which has the best reach if the mass gap between sbottom and neutralino is large. We have checked that the total number of backgrounds after the selection cuts, if normalized to $3.2\,\text{fb}^{-1}$, is in good agreement with Ref. [63]. We use the asymptotic formula for the significance in Ref. [79] (also adopted by Ref. [53, 54]),

$$\sigma = \sqrt{2\left[(s+b)\log\left(1+s/b\right) - s\right]}\,, \tag{4.1}$$

which reduces to the usual $s/\sqrt{b}$ in the limit $b \gg s$. While the optimal values of the selection cuts depend on the signal spectrum, for simplicity we fix the cuts as in Section 3. In particular, for the $\boldsymbol{2\ell + E_T^{miss}}$ channel the cuts we choose are relatively conservative to maintain a sufficiently large simulated signal sample. A more sophisticated optimization method could further improve the reach of the searches.

In Fig. 5, we show the expected exclusion regions for the three channels in the $(m_{\tilde{b}},\ \text{BR}(\tilde{b} \to \tilde{t}\,W))$ plane, assuming $m_{\tilde{b}} - m_{\tilde{t}} = 400\,\text{GeV}$ and $m_{\tilde{t}} - m_{\chi} = 30\,\text{GeV}$. On the left panel, the red, blue and green contours indicate the 2-sigma limits of the $\boldsymbol{2\ell + E_T^{miss}}$, $\boldsymbol{1b1\ell + E_T^{miss}}$ and $\boldsymbol{2b + E_T^{miss}}$ channels, respectively, and the corresponding shaded regions are excluded at 95% confidence level (CL). On the right panel, the 5-sigma reaches are shown instead. For the solid curves, we assume the stop only decays to charm and neutralino, $\tilde{t} \to c\,\chi$; for the dashed curves, we assume that the stop only goes through the 4-body decay, $\tilde{t} \to bW^*\chi \to bl\nu\chi/bjj\chi$. As we expected, the stop decay channel has a small impact on the reach. The complementarity of different channels is well demonstrated in Fig. 5. The $\boldsymbol{2\ell + E_T^{miss}}$ ($\boldsymbol{2b + E_T^{miss}}$) channel has the best reach if the decay $\tilde{b} \to \tilde{t}\,W$ ($\tilde{b} \to b\,\chi$) is dominant, and the $\boldsymbol{1b1\ell + E_T^{miss}}$ channel has a better reach if the branching ratio of the two decay channels are comparable. We also found that the $\boldsymbol{2b + E_T^{miss}}$ channel has rather good reaches, comparable to the reach of the $\boldsymbol{1b1\ell + E_T^{miss}}$ channel even for $\text{BR}(\tilde{b} \to \tilde{t}\,W) \sim 0.5$. Nevertheless, the $\boldsymbol{1b1\ell + E_T^{miss}}$ channel could still significantly improve the overall significance (of all channels combined) and impose constraints on the stop mass.

To determine the bounds on masses of sbottom and stop, we also show the 2-sigma

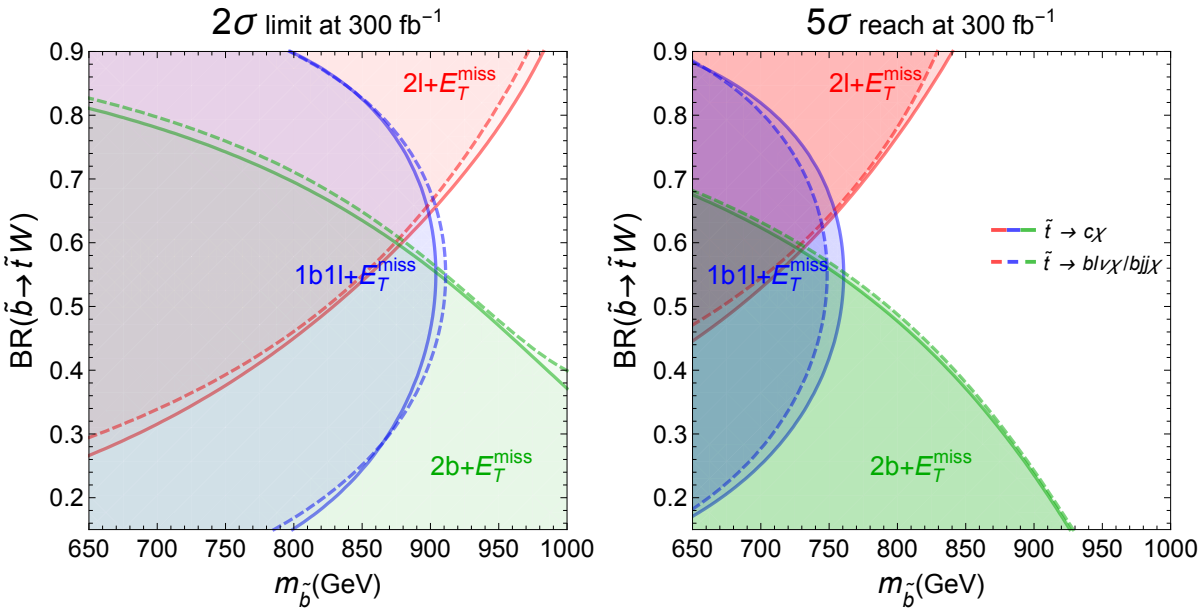

Figure 5: Expected $2\,\sigma$ limits (left) and $5\,\sigma$ reaches (right) in the $(m_{\tilde{b}},\ \mathrm{BR}(\tilde{b}\to\tilde{t}\,W))$ plane from the 13 TeV LHC with $300\,\mathrm{fb}^{-1}$ data, assuming $m_{\tilde{b}}-m_{\tilde{t}}=400\,\mathrm{GeV}$ and $m_{\tilde{t}}-m_{\chi}=30\,\mathrm{GeV}$. The red, blue and green contours indicate the regions excluded by the $\boldsymbol{2\ell+E_{\mathrm{T}}^{\mathrm{miss}}}$, $\boldsymbol{1b1\ell+E_{\mathrm{T}}^{\mathrm{miss}}}$ and $\boldsymbol{2b+E_{\mathrm{T}}^{\mathrm{miss}}}$ channels, respectively. The solid (dashed) curves corresponds to the stop decay $\tilde{t}\to c\,\chi$ ($\tilde{t}\to bW^{*}\chi\to bl\nu\chi/bjj\chi$) with 100% BR.

limits and 5-sigma reaches in the $(m_{\tilde{b}},\ m_{\tilde{b}}-m_{\tilde{t}})$ plane in Fig. 6 for $\mathrm{BR}(\tilde{b}\to\tilde{t}\,W)=0.9$ (top panel) and 0.5 (bottom panel), assuming $m_{\tilde{t}}-m_{\chi}=30\,\mathrm{GeV}$. A few benchmarks of stop masses are also shown, which correspond to diagonal lines in the $(m_{\tilde{b}},\ m_{\tilde{b}}-m_{\tilde{t}})$ plane. For $\mathrm{BR}(\tilde{b}\to\tilde{t}\,W)=0.9$, it is clear that the $\boldsymbol{2\ell+E_{\mathrm{T}}^{\mathrm{miss}}}$ channel has the best reach, and stop masses up to $\sim 600\,\mathrm{GeV}$ can be excluded for $m_{\tilde{b}}\lesssim 1\,\mathrm{TeV}$. For $\mathrm{BR}(\tilde{b}\to\tilde{t}\,W)=0.5$, the $\boldsymbol{1b1\ell+E_{\mathrm{T}}^{\mathrm{miss}}}$ and $\boldsymbol{2b+E_{\mathrm{T}}^{\mathrm{miss}}}$ channels have comparable reaches, with the $\boldsymbol{1b1\ell+E_{\mathrm{T}}^{\mathrm{miss}}}$ ($\boldsymbol{2b+E_{\mathrm{T}}^{\mathrm{miss}}}$) channel having better constraints on $m_{\tilde{t}}$ in the regions with smaller (larger) $m_{\tilde{b}}$. However, it should be noted that the $\boldsymbol{2b+E_{\mathrm{T}}^{\mathrm{miss}}}$ channel does not direct constrain $m_{\tilde{t}}$, and the exclusion region shown in Fig. 6 is based on the assumption $m_{\tilde{t}}-m_{\chi}=30\,\mathrm{GeV}$. For the $\boldsymbol{1b1\ell+E_{\mathrm{T}}^{\mathrm{miss}}}$ channel, stop masses up to $\sim 500\,\mathrm{GeV}$ can be excluded for $m_{\tilde{b}}\lesssim 900\,\mathrm{GeV}$. It should also be noted that in obtaining the constraints we have assumed a sufficient mass gap between the sbottom and the stop. If the mass gap is small, the search strategy can be drastically different, in particular in the region $m_{\tilde{b}}-m_{\tilde{t}}\lesssim m_W$. Further studies are required to determine the collider reach in this region.

Comparing to the reach of the direct stop search, the recent results from the ATLAS mono-jet search has excluded stop masses below 323 GeV with $3.2\,\mathrm{fb}^{-1}$ data at $\sqrt{s}=$

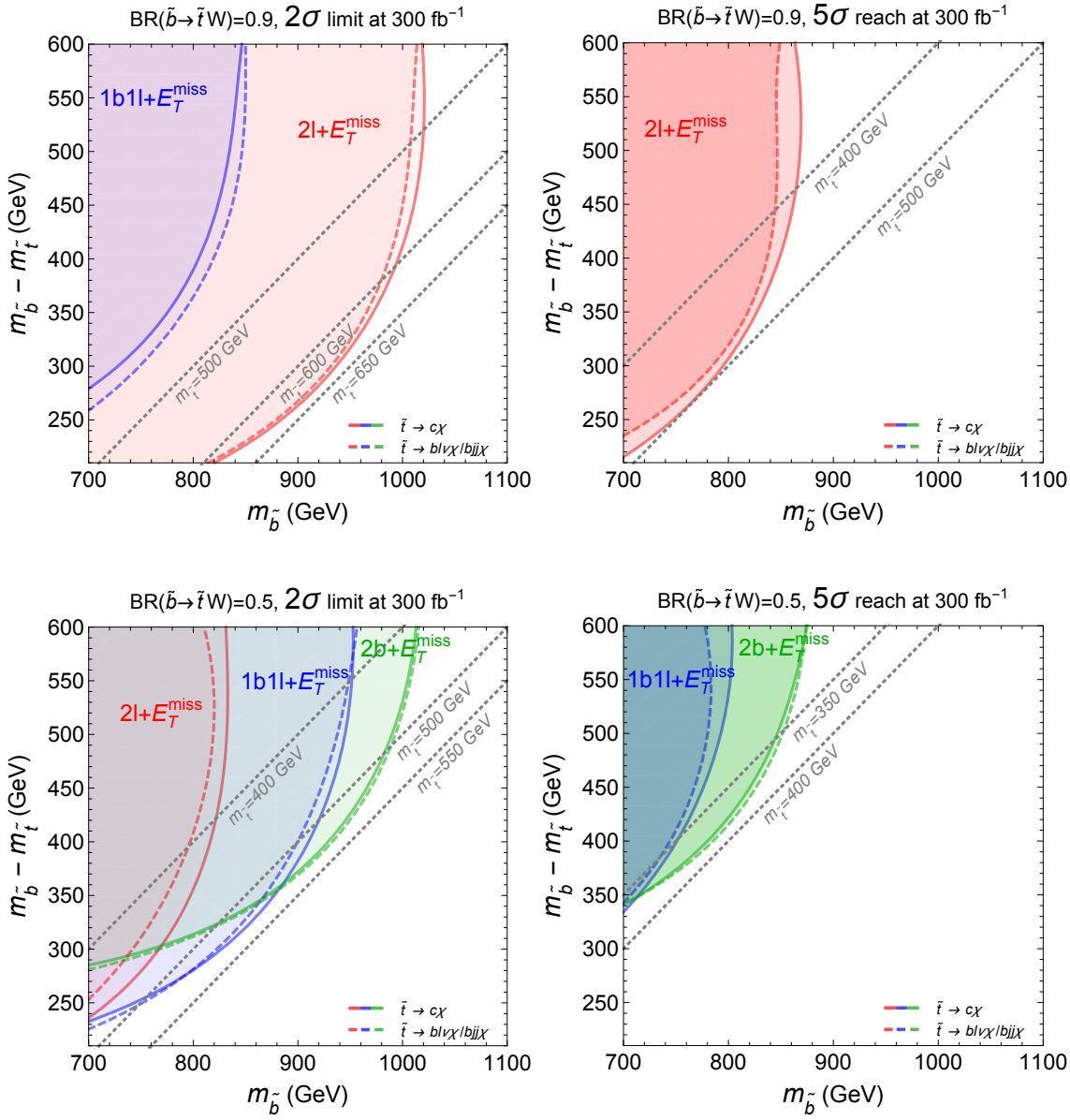

Figure 6: Expected $2\,\sigma$ limits (left) and $5\,\sigma$ reaches (right) in the $(m_{\tilde{b}},\ m_{\tilde{b}}-m_{\tilde{t}})$ plane from the 13 TeV LHC with 300 fb^{-1} data, assuming $m_{\tilde{t}}-m_{\chi}=30$ GeV. The top (bottom) panel assumes BR$(\tilde{b}\to\tilde{t}\,W)=0.9$ (0.5). The red, blue and green contours indicate the regions excluded by the $\boldsymbol{2\ell+E_T^{miss}}$, $\boldsymbol{1b1\ell+E_T^{miss}}$ and $\boldsymbol{2b+E_T^{miss}}$ channels, respectively. The solid (dashed) curves corresponds to the stop decay $\tilde{t}\to c\,\chi$ ($\tilde{t}\to bW^*\chi\to bl\nu\chi/bjj\chi$) with 100% BR. The dotted diagonal lines correspond to constant values of $m_{\tilde{t}}$.

13 TeV, assuming $m_{\tilde{t}} - m_\chi \approx 5\,\text{GeV}$ [57]. This already surpasses the constraints from the 8 TeV run [25, 26]. CMS conducted a search with $2.3\,\text{fb}^{-1}$ data at $\sqrt{s} = 13\,\text{TeV}$ using the α_T variable which can exclude stop masses up to 400 GeV assuming $m_{\tilde{t}} - m_\chi \approx 10\,\text{GeV}$ [58]. In both searches, the bounds on stop mass are also significantly weaker for slightly larger values of $m_{\tilde{t}} - m_\chi$. In Ref. [35], it is estimated that the high luminosity LHC with $3000\,\text{fb}^{-1}$ data at $\sqrt{s} = 14\,\text{TeV}$ is required for the bounds on stop mass from mono-jet search to reach $\sim 500\,\text{GeV}$, assuming the stop is in the coannihilation region. While the constraints from mono-jet searches do not rely on the properties of sbottom and are hence more robust, the search with sbottom decays could potentially have a much better reach. The two searches are also complementary; if a significant excess is found in the $\boldsymbol{2\ell + E_\text{T}^\text{miss}}$ or $\boldsymbol{1b1\ell + E_\text{T}^\text{miss}}$ channel, one may also expect a mild excess in the mono-jet search if the excess comes from a light stop in the coannihiliation region.

5 Conclusion

A light stop with mass almost degenerate with the lightest neutralino is an appealing SUSY scenario. It could evade the bounds of traditional stop searches and hence reduce the tension between naturalness and the current LHC results, while also having interesting implications for bino dark matter. In this paper, we propose a novel way of probing such stop particles by searching for it from sbottom decays, under the assumptions that the sbottom is not too heavy and has a significant branching ratio of decaying into a stop and a W boson ($\tilde{b} \to \tilde{t}\,W$). Such assumptions are favored by naturalness and Higgs mass considerations. In this scenario, the constraints on the masses of stop and sbottom from the traditional searches are weak. We show that a dedicated search for a sbottom pair with one or both sbottom decaying to stop and W at the 13 TeV LHC could impose strong constraint on this scenario, hence making it the optimal search channel. Assuming $m_{\tilde{t}} - m_\chi \approx 30\,\text{GeV}$, if the decay $\tilde{b} \to \tilde{t}\,W$ is dominant, the channel with final states $\boldsymbol{2\ell + E_\text{T}^\text{miss}}$ has the best reach, and can exclude stop masses up to $\sim 600\,\text{GeV}$ with $300\,\text{fb}^{-1}$ data if the sbottom is below 1 TeV; if the sbottom decays to either $\tilde{t}\,W$ or $b\,\chi$ with comparable branching ratios, the channel with final states $\boldsymbol{1b1\ell + E_\text{T}^\text{miss}}$ has a better reach and could exclude the stop with mass up to $\sim 500\,\text{GeV}$ with $300\,\text{fb}^{-1}$ data if the sbottom is below 900 GeV. While the results rely on the properties of the sbottom, the reaches are potentially much better than the one from direct searches of stop with mono-jet + E_T^miss final states, which could only reach up to $\sim 500\,\text{GeV}$ with $3000\,\text{fb}^{-1}$ data at

$\sqrt{s} = 14\,\text{TeV}$. The traditional search channel of sbottom with final states $\boldsymbol{2b + E_T^{miss}}$ is also complementary to the ones we propose. Together, these searches can cover a wide range of model parameter space and provide valuable information on the status of SUSY.

There are other interesting scenarios not explored in this paper but may worth further investigation. It is possible that the chargino or second neutralino are lighter than the sbottom, making its decay more complicated [80]. In this case, searching for the asymmetric decay chains with one sbottom decaying to $\tilde{t}W$, the other decaying to $t\chi^{\pm}$ or $b\chi_2$ could be useful. For larger values of the stop-neutralino mass gap, the stop decay products become more visible and it might be useful to look at channels with multiple b-jets or multiple leptons [54], or try to tag the charm quark from stop decay [23–25]. On the other hand, if the mass gap is smaller, the stop decay could exhibit displaced vertex, which can help reduce SM background in both the mono-jet search and the search with sbottom decays. It is also complementary to search for the lighter stop from the decays of the heavier stop [81–83].

Our study serves as a proof of concept. A search carried out by the LHC experimental groups is desired to fully determine the reach of the proposed channels. Since the $\boldsymbol{2\ell + E_T^{miss}}$ channel has been used to search for sleptons and electroweakinos, and the conventional search of stop in the semileptonic channel is very similar to the $\boldsymbol{1b1\ell + E_T^{miss}}$ channel we studied, reinterpretation of those search results can already lead to interesting reach. At the same time, optimizing the searches with these new channels in mind is needed to realize their full potential. While the current data is still not very constraining, in the future it is straightforward to interpret the results of conventional searches in these two channels in terms of constraints on the scenario studied in this paper. If deviations from the SM is observed, it is non-trivial to discriminate different new physics scenarios that leads to similar signals, and the comparisons between different search channels are important.

Acknowledgments

We would like to thank Zhen Liu for useful discussions. HA is supported by the Walter Burke Institute at Caltech and by DOE Grant de-sc0011632. JG is supported by the International Postdoctoral Exchange Fellowship Program between the Office of the National Administrative Committee of Postdoctoral Researchers of China (ONACPR) and DESY. JG would also like to express a special thanks to the Mainz Institute for Theoretical Physics (MITP) for its hospitality and support. LTW is supported by DOE grant

DE-SC0013642.

References

[1] **CMS** Collaboration, *Search for direct top squark pair production in the single lepton final state at* $\sqrt{s} = 13$ TeV, Tech. Rep. CMS-PAS-SUS-16-028, CERN, Geneva, 2016.

[2] **CMS** Collaboration, *Search for direct top squark pair production in the fully hadronic final state in proton-proton collisions at sqrt(s) = 13 TeV corresponding to an integrated luminosity of 12.9/fb*, Tech. Rep. CMS-PAS-SUS-16-029, CERN, Geneva, 2016.

[3] **CMS** Collaboration, *Search for supersymmetry in the all-hadronic final state using top quark tagging in pp collisions at sqrt(s) = 13 TeV*, Tech. Rep. CMS-PAS-SUS-16-030, CERN, Geneva, 2016.

[4] **ATLAS** Collaboration, *Search for top squarks in final states with one isolated lepton, jets, and missing transverse momentum in* $\sqrt{s}$ *= 13 TeV pp collisions with the ATLAS detector*, Tech. Rep. ATLAS-CONF-2016-050, CERN, Geneva, Aug, 2016.

[5] **ATLAS** Collaboration, *Search for the Supersymmetric Partner of the Top Quark in the Jets+Emiss Final State at sqrt(s) = 13 TeV*, Tech. Rep. ATLAS-CONF-2016-077, CERN, Geneva, Aug, 2016.

[6] **ATLAS** Collaboration, G. Aad et al., *ATLAS Run 1 searches for direct pair production of third-generation squarks at the Large Hadron Collider*, *Eur. Phys. J.* **C75** (2015), no. 10 510, [arXiv:1506.08616]. [Erratum: Eur. Phys. J.C76,no.3,153(2016)].

[7] **CMS** Collaboration, V. Khachatryan et al., *Search for direct pair production of scalar top quarks in the single- and dilepton channels in proton-proton collisions at* $\sqrt{s} = 8$ *TeV*, *JHEP* **07** (2016) 027, [arXiv:1602.03169]. [Erratum: JHEP09,056(2016)].

[8] **CMS** Collaboration, V. Khachatryan et al., *Search for direct pair production of supersymmetric top quarks decaying to all-hadronic final states in pp collisions at $\sqrt{s} = 8$ TeV*, *Eur. Phys. J.* **C76** (2016), no. 8 460, [arXiv:1603.00765].

[9] **CMS** Collaboration, *Search for direct top squark pair production in the single lepton final state at $\sqrt{s} = 13$ TeV*, Tech. Rep. CMS-PAS-SUS-16-002, CERN, Geneva, 2016.

[10] **CMS** Collaboration, J. Bradmiller-Feld, *Search for supersymmetry in the multijet and missing transverse momentum final state*, in *51st Rencontres de Moriond on EW Interactions and Unified Theories La Thuile, Italy, March 12-19, 2016*, 2016. arXiv:1605.05762.

[11] **ATLAS** Collaboration, M. Aaboud et al., *Search for top squarks in final states with one isolated lepton, jets, and missing transverse momentum in $\sqrt{s} = 13$ TeV pp collisions with the ATLAS detector*, *Phys. Rev.* **D94** (2016), no. 5 052009, [arXiv:1606.03903].

[12] M. Jezabek, *Top quark physics*, *Nucl. Phys. Proc. Suppl.* **37B** (1994), no. 2 197, [hep-ph/9406411].

[13] A. Brandenburg, Z. G. Si, and P. Uwer, *QCD corrected spin analyzing power of jets in decays of polarized top quarks*, *Phys. Lett.* **B539** (2002) 235–241, [hep-ph/0205023].

[14] Z. Han, A. Katz, D. Krohn, and M. Reece, *(Light) Stop Signs*, *JHEP* **08** (2012) 083, [arXiv:1205.5808].

[15] **CDF** Collaboration, T. Aaltonen et al., *Measurement of $t\bar{t}$ Spin Correlation in $p\bar{p}$ Collisions Using the CDF II Detector at the Tevatron*, *Phys. Rev.* **D83** (2011) 031104, [arXiv:1012.3093].

[16] **D0** Collaboration, V. M. Abazov et al., *Measurement of spin correlation in $t\bar{t}$ production using dilepton final states*, *Phys. Lett.* **B702** (2011) 16–23, [arXiv:1103.1871].

[17] **D0** Collaboration, V. M. Abazov et al., *Measurement of spin correlation in $t\bar{t}$ production using a matrix element approach*, *Phys. Rev. Lett.* **107** (2011) 032001, [arXiv:1104.5194].

[18] **D0** Collaboration, V. M. Abazov et al., *Measurement of the top quark pair production cross section in the lepton+jets channel in proton-antiproton collisions at $\sqrt{s}$=1.96 TeV*, *Phys. Rev.* **D84** (2011) 012008, [arXiv:1101.0124].

[19] **ATLAS** Collaboration, G. Aad et al., *Observation of spin correlation in $t\bar{t}$ events from pp collisions at sqrt(s) = 7 TeV using the ATLAS detector*, *Phys. Rev. Lett.* **108** (2012) 212001, [arXiv:1203.4081].

[20] **ATLAS** Collaboration, G. Aad et al., *Measurements of spin correlation in top-antitop quark events from proton-proton collisions at $\sqrt{s} = 7$ TeV using the ATLAS detector*, *Phys. Rev.* **D90** (2014), no. 11 112016, [arXiv:1407.4314].

[21] **CMS** Collaboration, S. Chatrchyan et al., *Measurements of $t\bar{t}$ spin correlations and top-quark polarization using dilepton final states in pp collisions at $\sqrt{s} = 7$ TeV*, *Phys. Rev. Lett.* **112** (2014), no. 18 182001, [arXiv:1311.3924].

[22] **ATLAS** Collaboration, G. Aad et al., *Measurement of Spin Correlation in Top-Antitop Quark Events and Search for Top Squark Pair Production in pp Collisions at $\sqrt{s} = 8$ TeV Using the ATLAS Detector*, *Phys. Rev. Lett.* **114** (2015), no. 14 142001, [arXiv:1412.4742].

[23] A. Choudhury and A. Datta, *New limits on top squark NLSP from LHC 4.7 fb^{-1} data*, *Mod. Phys. Lett.* **A27** (2012) 1250188, [arXiv:1207.1846].

[24] G. Belanger, D. Ghosh, R. Godbole, M. Guchait, and D. Sengupta, *Probing the flavor violating scalar top quark signal at the LHC*, *Phys. Rev.* **D89** (2014) 015003, [arXiv:1308.6484].

[25] **ATLAS** Collaboration, G. Aad et al., *Search for pair-produced third-generation squarks decaying via charm quarks or in compressed supersymmetric scenarios in pp collisions at $\sqrt{s} = 8$ TeV with the ATLAS detector*, *Phys. Rev.* **D90** (2014), no. 5 052008, [arXiv:1407.0608].

[26] **CMS** Collaboration, V. Khachatryan et al., *Search for top squark pair production in compressed-mass-spectrum scenarios in proton-proton collisions at sqrt(s) = 8 TeV using the alphaT variable*, *Submitted to: Phys. Lett. B* (2016) [arXiv:1605.08993].

[27] M. Carena, A. Freitas, and C. E. M. Wagner, *Light Stop Searches at the LHC in Events with One Hard Photon or Jet and Missing Energy*, *JHEP* **10** (2008) 109, [arXiv:0808.2298].

[28] S. Bornhauser, M. Drees, S. Grab, and J. S. Kim, *Light Stop Searches at the LHC in Events with two b-Jets and Missing Energy*, *Phys. Rev.* **D83** (2011) 035008, [arXiv:1011.5508].

[29] M. A. Ajaib, T. Li, and Q. Shafi, *Stop-Neutralino Coannihilation in the Light of LHC*, *Phys. Rev.* **D85** (2012) 055021, [arXiv:1111.4467].

[30] M. Drees, M. Hanussek, and J. S. Kim, *Light Stop Searches at the LHC with Monojet Events*, *Phys. Rev.* **D86** (2012) 035024, [arXiv:1201.5714].

[31] H. Dreiner, M. Krmer, and J. Tattersall, *Exploring QCD uncertainties when setting limits on compressed supersymmetric spectra*, *Phys. Rev.* **D87** (2013), no. 3 035006, [arXiv:1211.4981].

[32] K. Krizka, A. Kumar, and D. E. Morrissey, *Very Light Scalar Top Quarks at the LHC*, *Phys. Rev.* **D87** (2013), no. 9 095016, [arXiv:1212.4856].

[33] A. Delgado, G. F. Giudice, G. Isidori, M. Pierini, and A. Strumia, *The light stop window*, *Eur. Phys. J.* **C73** (2013), no. 3 2370, [arXiv:1212.6847].

[34] T. Cohen, T. Golling, M. Hance, A. Henrichs, K. Howe, J. Loyal, S. Padhi, and J. G. Wacker, *A Comparison of Future Proton Colliders Using SUSY Simplified Models: A Snowmass Whitepaper*, in *Community Summer Study 2013: Snowmass on the Mississippi (CSS2013) Minneapolis, MN, USA, July 29-August 6, 2013*, 2013. arXiv:1310.0077.

[35] M. Low and L.-T. Wang, *Neutralino dark matter at 14 TeV and 100 TeV*, *JHEP* **08** (2014) 161, [arXiv:1404.0682].

[36] G. Ferretti, R. Franceschini, C. Petersson, and R. Torre, *Spot the stop with a b-tag*, *Phys. Rev. Lett.* **114** (2015) 201801, [arXiv:1502.01721].

[37] **CMS** Collaboration, V. Khachatryan et al., *Searches for third-generation squark production in fully hadronic final states in proton-proton collisions at* $\sqrt{s} = 8$ *TeV*, *JHEP* **06** (2015) 116, [arXiv:1503.08037].

[38] K.-i. Hikasa, J. Li, L. Wu, and J. M. Yang, *Single top squark production as a probe of natural supersymmetry at the LHC*, *Phys. Rev.* **D93** (2016), no. 3 035003, [arXiv:1505.06006].

[39] M. Czakon, A. Mitov, M. Papucci, J. T. Ruderman, and A. Weiler, *Closing the stop gap*, *Phys. Rev. Lett.* **113** (2014), no. 20 201803, [arXiv:1407.1043].

[40] **ATLAS** Collaboration, G. Aad et al., *Measurement of the $t\bar{t}$ production cross-section using $e\mu$ events with b -tagged jets in pp collisions at $\sqrt{s} = 7$ and 8 TeV with the ATLAS detector*, *Eur. Phys. J.* **C74** (2014), no. 10 3109, [arXiv:1406.5375].

[41] K. Rolbiecki and J. Tattersall, *Refining light stop exclusion limits with W^+W^- cross sections*, *Phys. Lett.* **B750** (2015) 247–251, [arXiv:1505.05523].

[42] B. Dutta, W. Flanagan, A. Gurrola, W. Johns, T. Kamon, P. Sheldon, K. Sinha, K. Wang, and S. Wu, *Probing compressed top squark scenarios at the LHC at 14 TeV*, *Phys. Rev.* **D90** (2014), no. 9 095022, [arXiv:1312.1348].

[43] M. Drees and M. M. Nojiri, *A new signal for scalar top bound state production*, *Phys. Rev. Lett.* **72** (1994) 2324–2327, [hep-ph/9310209].

[44] M. Drees and M. M. Nojiri, *Production and decay of scalar stoponium bound states*, *Phys. Rev.* **D49** (1994) 4595–4616, [hep-ph/9312213].

[45] S. P. Martin, *Diphoton decays of stoponium at the Large Hadron Collider*, *Phys. Rev.* **D77** (2008) 075002, [arXiv:0801.0237].

[46] B. Batell and S. Jung, *Probing Light Stops with Stoponium*, *JHEP* **07** (2015) 061, [arXiv:1504.01740].

[47] R. Gröber, M. M. Mühlleitner, E. Popenda, and A. Wlotzka, *Light Stop Decays: Implications for LHC Searches*, *Eur. Phys. J.* **C75** (2015) 420, [arXiv:1408.4662].

[48] D. S. M. Alves, M. R. Buckley, P. J. Fox, J. D. Lykken, and C.-T. Yu, *Stops and $\not{E}_T$: The shape of things to come*, *Phys. Rev.* **D87** (2013), no. 3 035016, [arXiv:1205.5805].

[49] K. Hagiwara and T. Yamada, *Equal-velocity scenario for hiding dark matter at the LHC*, *Phys. Rev.* **D91** (2015), no. 9 094007, [arXiv:1307.1553].

[50] H. An and L.-T. Wang, *Opening up the compressed region of top squark searches at 13 TeV LHC*, *Phys. Rev. Lett.* **115** (2015) 181602, [arXiv:1506.00653].

[51] S. Macaluso, M. Park, D. Shih, and B. Tweedie, *Revealing Compressed Stops Using High-Momentum Recoils*, *JHEP* **03** (2016) 151, [arXiv:1506.07885].

[52] A. Kobakhidze, N. Liu, L. Wu, J. M. Yang, and M. Zhang, *Closing up a light stop window in natural SUSY at LHC*, *Phys. Lett.* **B755** (2016) 76–81, [arXiv:1511.02371].

[53] H.-C. Cheng, C. Gao, L. Li, and N. A. Neill, *Stop Search in the Compressed Region via Semileptonic Decays*, *JHEP* **05** (2016) 036, [arXiv:1604.00007].

[54] H.-C. Cheng, L. Li, and Q. Qin, *Second Stop and Sbottom Searches with a Stealth Stop*, arXiv:1607.06547.

[55] P. Jackson, C. Rogan, and M. Santoni, *Sparticles in Motion - getting to the line in compressed scenarios with the Recursive Jigsaw Reconstruction*, arXiv:1607.08307.

[56] B. Kaufman, P. Nath, B. D. Nelson, and A. B. Spisak, *Light Stops and Observation of Supersymmetry at LHC RUN-II*, *Phys. Rev.* **D92** (2015) 095021, [arXiv:1509.02530].

[57] **ATLAS** Collaboration, M. Aaboud et al., *Search for new phenomena in final states with an energetic jet and large missing transverse momentum in pp collisions at* $\sqrt{s} = 13$ *TeV using the ATLAS detector*, arXiv:1604.07773.

[58] **CMS** Collaboration, V. Khachatryan et al., *A search for new phenomena in pp collisions at sqrt(s) = 13 TeV in final states with missing transverse momentum and at least one jet using the alphaT variable*, arXiv:1611.00338.

[59] D. Goncalves, K. Sakurai, and M. Takeuchi, *Tagging a mono-top signature in Natural SUSY*, arXiv:1610.06179.

[60] J. R. Ellis, K. A. Olive, and Y. Santoso, *Calculations of neutralino stop coannihilation in the CMSSM*, *Astropart. Phys.* **18** (2003) 395–432, [hep-ph/0112113].

[61] A. Berlin, D. S. Robertson, M. P. Solon, and K. M. Zurek, *Bino variations: Effective field theory methods for dark matter direct detection*, *Phys. Rev.* **D93** (2016), no. 9 095008, [arXiv:1511.05964].

[62] G. Blanger, F. Boudjema, A. Pukhov, and A. Semenov, *micrOMEGAs4.1: two dark matter candidates*, *Comput. Phys. Commun.* **192** (2015) 322–329, [arXiv:1407.6129].

[63] **ATLAS** Collaboration, M. Aaboud et al., *Search for bottom squark pair production in proton–proton collisions at $\sqrt{s}$ =13 TeV with the ATLAS detector*, arXiv:1606.08772.

[64] **ATLAS** Collaboration, G. Aad et al., *Search for direct production of charginos, neutralinos and sleptons in final states with two leptons and missing transverse momentum in pp collisions at $\sqrt{s}$ = 8 TeV with the ATLAS detector*, *JHEP* **05** (2014) 071, [arXiv:1403.5294].

[65] **CMS** Collaboration, V. Khachatryan et al., *Searches for electroweak production of charginos, neutralinos, and sleptons decaying to leptons and W, Z, and Higgs bosons in pp collisions at 8 TeV*, *Eur. Phys. J.* **C74** (2014), no. 9 3036, [arXiv:1405.7570].

[66] J. Alwall, M. Herquet, F. Maltoni, O. Mattelaer, and T. Stelzer, *MadGraph 5 : Going Beyond*, *JHEP* **06** (2011) 128, [arXiv:1106.0522].

[67] T. Sjostrand, S. Mrenna, and P. Z. Skands, *PYTHIA 6.4 Physics and Manual*, *JHEP* **05** (2006) 026, [hep-ph/0603175].

[68] **DELPHES 3** Collaboration, J. de Favereau, C. Delaere, P. Demin, A. Giammanco, V. Lematre, A. Mertens, and M. Selvaggi, *DELPHES 3, A modular framework for fast simulation of a generic collider experiment*, *JHEP* **02** (2014) 057, [arXiv:1307.6346].

[69] *Expected performance of the ATLAS b-tagging algorithms in Run-2*, Tech. Rep. ATL-PHYS-PUB-2015-022, CERN, Geneva, Jul, 2015.

[70] C. Borschensky, M. Krämer, A. Kulesza, M. Mangano, S. Padhi, T. Plehn, and X. Portell, *Squark and gluino production cross sections in pp collisions at $\sqrt{s}$ = 13, 14, 33 and 100 TeV*, *Eur. Phys. J.* **C74** (2014), no. 12 3174, [arXiv:1407.5066].

[71] S. Padhi, "Susycrosssections13tevstopsbottom, https://twiki.cern.ch/twiki/bin/view/LHCPhysics/SUSYCrossSections13TeVstopsbottom."

[72] M. Czakon and A. Mitov, *Top++: A Program for the Calculation of the Top-Pair Cross-Section at Hadron Colliders*, *Comput. Phys. Commun.* **185** (2014) 2930, [arXiv:1112.5675].

[73] "NNLO+NNLL top-quark-pair cross sections, https://twiki.cern.ch/twiki/bin/view/LHCPhysics/TtbarNNLO."

[74] J. M. Campbell, R. K. Ellis, and C. Williams, *Vector boson pair production at the LHC*, *JHEP* **07** (2011) 018, [arXiv:1105.0020].

[75] **ATLAS** Collaboration, M. Aaboud et al., *Measurement of the $t\bar{t}Z$ and $t\bar{t}W$ production cross sections in multilepton final states using 3.2 fb^{-1} of pp collisions at $\sqrt{s}$ = 13 TeV with the ATLAS detector*, arXiv:1609.01599.

[76] Y. Bai, H.-C. Cheng, J. Gallicchio, and J. Gu, *Stop the Top Background of the Stop Search*, *JHEP* **07** (2012) 110, [arXiv:1203.4813].

[77] **ATLAS** Collaboration, G. Aad et al., *Search for top squark pair production in final states with one isolated lepton, jets, and missing transverse momentum in $\sqrt{s}$ =8 TeV pp collisions with the ATLAS detector*, *JHEP* **11** (2014) 118, [arXiv:1407.0583].

[78] M. L. Graesser and J. Shelton, *Hunting Mixed Top Squark Decays*, *Phys. Rev. Lett.* **111** (2013), no. 12 121802, [arXiv:1212.4495].

[79] G. Cowan, K. Cranmer, E. Gross, and O. Vitells, *Asymptotic formulae for likelihood-based tests of new physics*, *Eur. Phys. J.* **C71** (2011) 1554, [arXiv:1007.1727]. [Erratum: Eur. Phys. J.C73,2501(2013)].

[80] T. Han, S. Su, Y. Wu, B. Zhang, and H. Zhang, *Sbottom discovery via mixed decays at the LHC*, *Phys. Rev.* **D92** (2015), no. 11 115009, [arXiv:1507.04006].

[81] M. Perelstein and C. Spethmann, *A Collider signature of the supersymmetric golden region*, *JHEP* **04** (2007) 070, [hep-ph/0702038].

[82] D. Ghosh, *Boosted dibosons from mixed heavy top squarks*, *Phys. Rev.* **D88** (2013), no. 11 115013, [arXiv:1308.0320].

[83] **CMS** Collaboration, V. Khachatryan et al., *Search for top-squark pairs decaying into Higgs or Z bosons in pp collisions at $\sqrt{s}$=8 TeV*, *Phys. Lett.* **B736** (2014) 371–397, [arXiv:1405.3886].